



## Short communication

One-pot synthesis of  $\text{NiFe}_2\text{O}_4/\text{C}$  composite as an anode material for lithium-ion batteriesYu Ding<sup>a,b</sup>, Yifu Yang<sup>a,\*</sup>, Huixia Shao<sup>a</sup><sup>a</sup> College of Chemistry and Molecular Sciences, Wuhan University, Wuhan 430072, PR China<sup>b</sup> College of Chemistry and Materials Science, Hubei Engineering University, Xiaogan 432000, PR China

## H I G H L I G H T S

- ▶ A nanostructured  $\text{NiFe}_2\text{O}_4/\text{C}$  is synthesized via the polymer pyrolysis method for lithium-ion batteries.
- ▶ The size range of the as-synthesized particles is approximately 50–100 nm.
- ▶ The obtained sample retains about 780 mAh  $\text{g}^{-1}$  after 40 cycles.
- ▶ The reversible capacity is over 200 mAh  $\text{g}^{-1}$  at the high rate of 4C.

## A R T I C L E I N F O

## Article history:

Received 30 October 2012

Received in revised form

5 January 2013

Accepted 8 January 2013

Available online 16 January 2013

## Keywords:

Nickel ferrite composite

Anode

Polymer pyrolysis method

Lithium-ion batteries

## A B S T R A C T

A simple polymer pyrolysis method for the synthesis of hierarchically nanostructured  $\text{NiFe}_2\text{O}_4/\text{C}$  composites is reported in this study. The characteristics of the material are examined by thermogravimetry, X-ray diffraction and scanning electron microscopy. The electrochemical performances of the nano-material composites are investigated in detail. The results show that the obtained composite retains a high specific capacity of 780 mAh  $\text{g}^{-1}$  even after 40 cycles at a current density of 1/8C, and the coulombic efficiency approaches 99%. The reversible specific capacity can still be as high as 200 mAh  $\text{g}^{-1}$ , at high rate of 4C. The nanostructured  $\text{NiFe}_2\text{O}_4/\text{C}$  composite is a potential competitive anode for lithium-ion batteries.

© 2013 Elsevier B.V. All rights reserved.

## 1. Introduction

Owing to the high operating voltage, high energy density, low self-discharge rate and long service life, rechargeable lithium-ion batteries (LIBs) are extremely promising power sources for various electronic devices [1–5]. However, the performance of rechargeable LIBs strongly depends on electrode materials, and the hunt for nanostructured high performance LIBs electrode materials remains the main research objectives [6–10]. Recently, nanostructured Fe-based ferrites with higher specific capacities have been explored as anode material in LIBs [11–17]. Unfortunately, the batteries using such materials display very rapid capacity fading during charge and discharge cycling. As a number of Fe-based ferrites,  $\text{NiFe}_2\text{O}_4$  have displayed a good electrochemical behavior and

a high theoretical capacity (914 mAh  $\text{g}^{-1}$ ). However, the vital limiting factors in the applicability of  $\text{NiFe}_2\text{O}_4$  are the rate of diffusion of lithium ion in the bulk material, low conductivity, and the large volume expansion and contraction during lithium insertion and extraction processes [11,18–20]. There has been growing evidence that nanostructured materials have improved electrochemical performances with respect to their bulk counterparts [21–23]. Thus, nanomaterial design and preparation strategy are crucial to improve further the electrochemical performance of  $\text{NiFe}_2\text{O}_4$  for LIBs. Furthermore, many reports have revealed that the carbon matrix has commonly been used as an elastic layer for buffering the volumetric changes and as a conductive additive for enhancing the electric conductivity [24–27]. Therefore, based on our previous works [17,28], a simple polymer pyrolysis method was used to synthesize hierarchically nanostructured  $\text{NiFe}_2\text{O}_4/\text{C}$  composites. The generated nanomaterials were thoroughly characterized by different techniques, and the electrochemical performances were also systematically investigated.

\* Corresponding author. Tel.: +86 27 68756765; fax: +86 27 68754067.  
E-mail address: [yang-yf1@vip.sina.com](mailto:yang-yf1@vip.sina.com) (Y. Yang).

## 2. Experimental

The polymeric precursor was prepared by solution polymerization of a mixed aqueous solution of acrylic acid in the presence of  $\text{Ni}(\text{NO}_3)_2 \cdot 6\text{H}_2\text{O}$  and  $\text{Fe}(\text{NO}_3)_3 \cdot 9\text{H}_2\text{O}$  with  $(\text{NH}_4)_2\text{S}_2\text{O}_8$  as the initiator. The molar fraction of Ni/Fe was fixed at 1:2.  $\text{Ni}(\text{NO}_3)_2 \cdot 6\text{H}_2\text{O}$  (0.01 mmol) and  $\text{Fe}(\text{NO}_3)_3 \cdot 9\text{H}_2\text{O}$  (0.02 mmol) were dissolved in 10 g acrylic acid solution (acrylic acid: $\text{H}_2\text{O}$  = 70:30 wt%) while stirring. A small amount (1 mL) of 5 wt%  $(\text{NH}_4)_2\text{S}_2\text{O}_8$  aqueous solution was added to the mixed acrylic acid solution to promote polymerization. Under heating at 80 °C for 1 h, the mixed solution was dried to form a well-distributed polyacrylate salt. The obtained polyacrylates were dried at 120 °C for 6 h, annealed at 800 °C for 2 h in nitrogen flow, and cooled at room temperature (NiFe-raw), and 450 °C in air for 8 h to obtain the  $\text{NiFe}_2\text{O}_4/\text{C}$  composites.

Electrochemical characterizations were performed using CR2016 coin cells with a Land BT2000 battery tester (Wuhan, China). The anode has a geometrical area of 2 cm<sup>2</sup> and consisted of 70 wt% active powder (as the active material) with 20 wt% acetylene black and 10 wt% polytetrafluoroethylene (PTFE). Acetylene black (Lizhiyuan KS6, Taiyuan, China) was intended to improve the electronic conductivity. The polymer was added to enhance the mechanical properties and to ensure the adherence of the material on the stainless steel mesh. The electrode was prepared by mixing the powder, acetylene black, and PTFE emulsion to form an electrode paste and rolling into a 0.1-mm-thick film. The electrode film was then pressed into a piece of 1-cm-diameter stainless steel mesh. The electrode was dried at 120 °C and 7 mbar for 4 h and pressed with a pressure of 1 ton cm<sup>-2</sup> to ensure a uniform surface. The test cells were assembled in an argon-filled glove box with 1 mol L<sup>-1</sup> solution of  $\text{LiPF}_6$  in ethylene carbonate/dimethyl carbonate (EC:DMC = 1:1 v/v) as the electrolyte. Fresh Li foil and Celgard 2300 were used as counter electrode and separator, respectively. The cell was galvanostatically cycled between 0.01 and 3.0 V (vs.  $\text{Li}^+/\text{Li}$ ), unless otherwise specified. A 3-electrode cell with Li foils was used as the counter and reference electrodes for cyclic voltammetry (CV) and electrochemical impedance spectroscopy (EIS) analyses. CV testing was performed on a CHI 660B Electrochemical Workstation (Chenghua, Shanghai, China) at a scan rate of 0.1 mV s<sup>-1</sup> between 0.01 and 3.0 V. The oscillation voltage applied to the cells and the frequency ranges were 5 mV and 100 kHz–0.1 Hz in the EIS measurements, respectively.

The thermogravimetry and differential thermogravimetry (TG–DTG) analyses were performed with a simultaneous SDT Q600 thermal analyzer to determine the exact decomposition temperature of the precursor. The conditions were 10 °C min<sup>-1</sup> from room temperature to 600 °C in air with a flow rate of 20 mL min<sup>-1</sup>. The

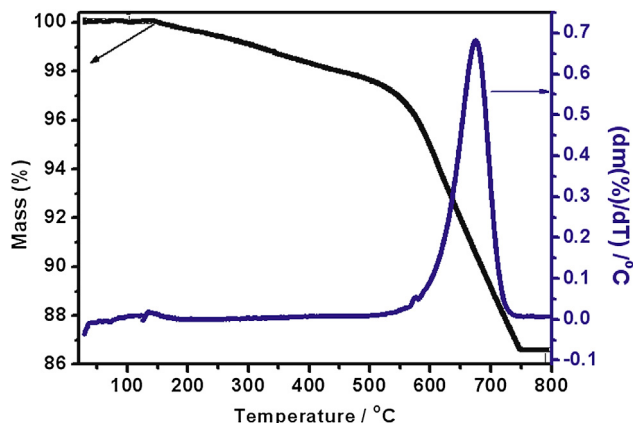


Fig. 1. Typical TG–DTG curves of the NiFe-raw precursor.

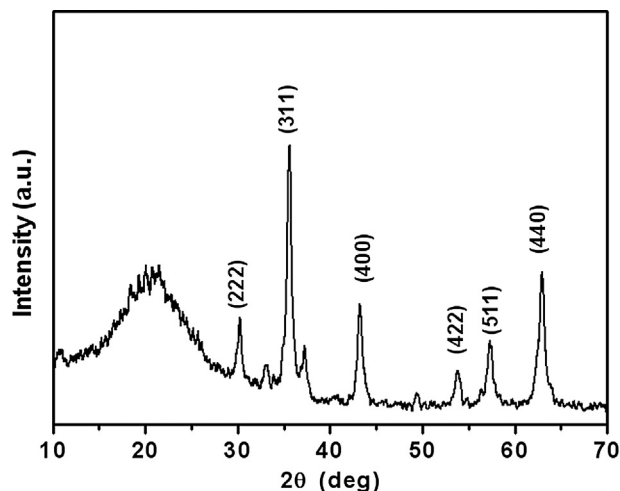


Fig. 2. X-ray diffraction pattern of  $\text{NiFe}_2\text{O}_4/\text{C}$ .

structures of the samples were analyzed by X-ray powder diffraction (XRD) by using a Shimadzu XRD-6000 diffractometer, in the  $2\theta$  range of 10.00°–70.00°, at the scan rate 2° min<sup>-1</sup>. The morphologies of the samples were examined using a scanning electron microscope (SEM, JSM-6700F scanning electron microscope).

## 3. Results and discussion

The amount of heat evolved or absorbed by the sample during the synthesis was monitored by TG. The thermograms of  $\text{NiFe}_2\text{O}_4/\text{C}$  obtained in air flow were shown in Fig. 1. The product had one weight loss process, and the weight loss was 13.4%, which was caused by the loss of carbon. Elemental analysis results showed that the carbon content was 13.34%. As shown in Fig. 2, the XRD analysis result indicates that the powders were a phase-pure cubic  $\text{NiFe}_2\text{O}_4$  (JCPDS card No.10-0325) [29]. The morphology of the final powder of  $\text{NiFe}_2\text{O}_4/\text{C}$  composites evaluated using SEM is shown in Fig. 3. The nanocrystalline particles were approximately 50 nm–100 nm in diameter.

The cyclic voltammetry (CV) profiles of the  $\text{NiFe}_2\text{O}_4/\text{C}$  composites for the first five cycles in the voltage range of 0.01 V–3.0 V versus  $\text{Li}/\text{Li}^+$  at a scan rate of 0.1 mV s<sup>-1</sup> are shown in Fig. 4. The broad peak was centered at 0.59 V in the first cathodic process,

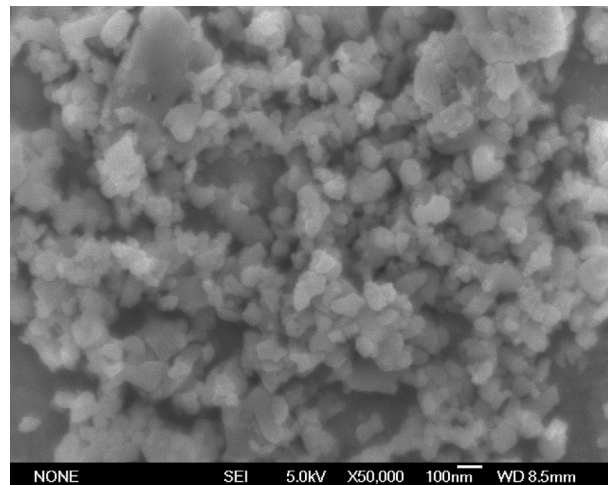


Fig. 3. SEM image of  $\text{NiFe}_2\text{O}_4/\text{C}$ .

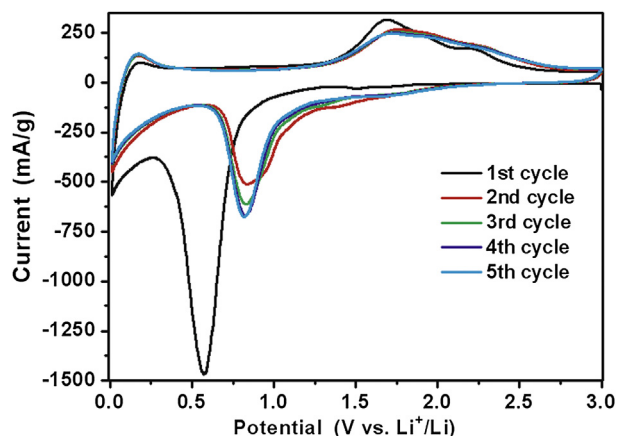


Fig. 4. Cyclic voltammograms of NiFe<sub>2</sub>O<sub>4</sub>/C (0.1 mV s<sup>-1</sup>, 0.01–3.0 V).

which could be originated from the reduction of Ni<sup>2+</sup> and Fe<sup>3+</sup> to Ni<sup>0</sup> and Fe<sup>0</sup>, and an irreversible reaction, was related to the decomposition of the electrolyte [30]. In the subsequent cycles, the main cathodic peak shifted to 0.86 V, which distinguishes the latter reduction mechanism from the one in the first cycle. The anodic peak at 1.8 V was observed in the first cycle and was attributed to the oxidation of the metallic iron and nickel into Fe<sup>3+</sup> and Ni<sup>2+</sup>, respectively [11,18–20,31], which did not obviously shift in the subsequent cycles.

The impedances of Li/NiFe<sub>2</sub>O<sub>4</sub>–C cells in the fresh lithiation, and delithiation processes states are shown in Fig. 5. The charge transfer resistance ( $R_{ct}$ ) maintained was very low, which may be attributed to the carbon matrix and the hierarchically nanostructured in the composite. The cell resistance increased after 10 cycles, but was also very low, which can be explained by the good electrochemical performance of the cell.

The cycling performances of the sample in different discharge–charge cycles are shown in Fig. 6(a). The lithiation capacity is 1230 mAh g<sup>-1</sup> in the first cycle. The discharge and charge capacities stabilized with a high coulombic efficiency, at the beginning of the second cycle. A reversible specific capacity of 780 mAh g<sup>-1</sup> can be obtained after 40 cycles at a constant current density of 1/8C, and the coulombic efficiency approaches 99% (Fig. 6(b)).

The observed high and stable specific capacity of the sample encourages studies on rate capabilities by using various current

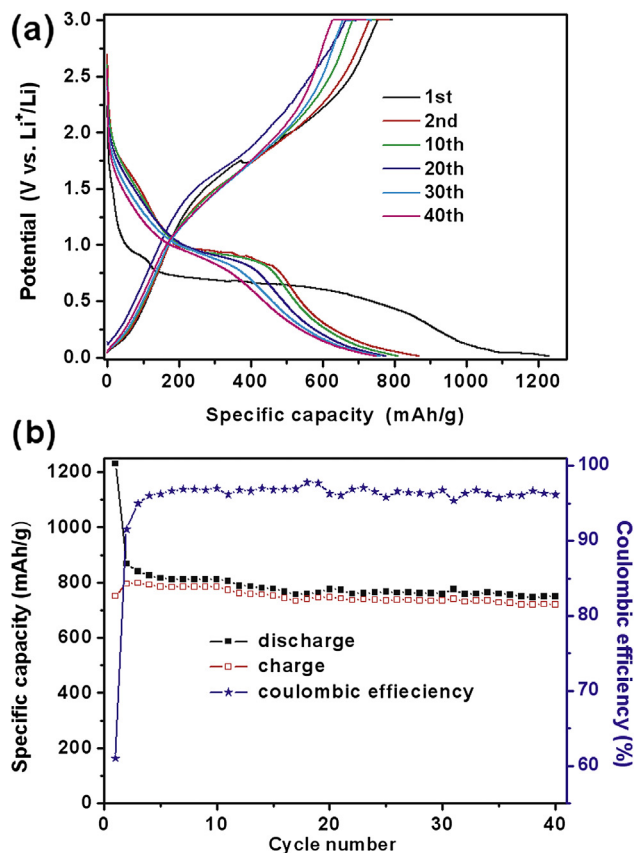


Fig. 6. (a) Charge–discharge voltage profiles. (b) Plot of capacity, coulombic efficiency vs. cycle number of NiFe<sub>2</sub>O<sub>4</sub>/C (0.01–3.0 V, 1/8C).

densities at ambient temperature. The lithiation capacities at different current densities of 0.2C–4C range are shown in Fig. 7. The currents were increased in several steps after every 10 cycles from 0.2C to 4C. The current density abruptly decreased to 0.2C after it was gradually increased to 4C. The capacity values decreased with increasing current rate. At a high rate of 4C (full discharge/charge of the active materials within 15 min, i.e., 3656 mA g<sup>-1</sup>), the reversible capacities of NiFe<sub>2</sub>O<sub>4</sub>/C were maintained as high as 200 mAh g<sup>-1</sup>. The results were highly attractive promising compared with other

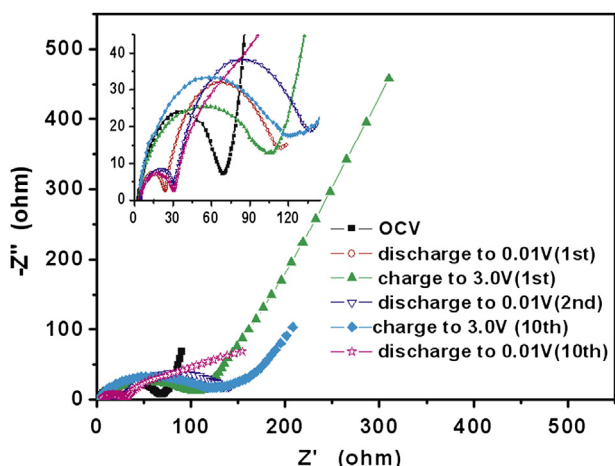


Fig. 5. Nyquist plots of Li/NiFe<sub>2</sub>O<sub>4</sub>–C cells.

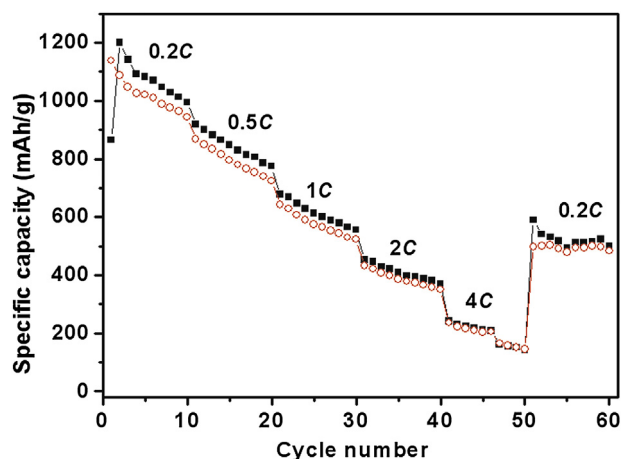


Fig. 7. Plot of capacity vs. cycle number of nanocrystalline NiFe<sub>2</sub>O<sub>4</sub>/C electrode at various current rates.

high-performance nanostructured anode materials [18–20,31]. The capacity increased to 600 mAh g<sup>-1</sup>, when the current rate was decreased from 4C to 0.2C. The results demonstrated that NiFe<sub>2</sub>O<sub>4</sub>/C has good rate capability, stability, and satisfactory capacity at each current density.

#### 4. Conclusions

A simple, scalable and highly reproducible process was presented for the preparation of a new hierarchically nanostructured NiFe<sub>2</sub>O<sub>4</sub>/C composite anode material. The material has a high specific capacity in the initial process and excellent retention even after 40 cycles. The galvanostatic cycling at different current rates revealed a specific capacity of 200 mAh g<sup>-1</sup> at 4C rate. This material has good potential as a competitive anode for LIBs.

#### Acknowledgments

This work was supported by the National Science Foundation of Hubei Province (No. 2012FFB00502 and 2012FFB00503).

#### References

- [1] S. Zugmann, D. Moosbauer, M. Amereller, C. Schreiner, F. Wudy, R. Schmitz, R. Schmitz, P. Isken, C. Dippel, R. Müller, M. Kunze, A. Lex-Balducci, M. Winter, H.J. Gores, J. Power Sources 196 (2011) 1417–1424.
- [2] G. Zhou, D.W. Wang, F. Li, L. Zhang, N. Li, Z.S. Wu, L. Wen, G.Q. Lu, H.M. Cheng, Chem. Mater. 22 (2010) 5306–5313.
- [3] Y.H. Xu, Rare Met. Mater. Eng. 32 (2003) 875–879.
- [4] J.B. Goodenough, Y. Kim, Chem. Mater. 22 (2010) 587–603.
- [5] J.B. Goodenough, Y. Kim, Chem. Mater. 22 (2009) 587–603.
- [6] Y. Zou, Y. Wang, ACS Nano 5 (2011) 8108–8114.
- [7] X. Zhu, Y. Zhu, S. Murali, M.D. Stoller, R.S. Ruoff, ACS Nano 5 (2011) 3333–3338.
- [8] S. Yoon, A. Manthiram, Electrochim. Acta 56 (2011) 3029–3035.
- [9] Z.G. Yang, D. Choi, S. Kerisit, K.M. Rosso, D.H. Wang, J. Zhang, G. Graff, J. Liu, J. Power Sources 192 (2009) 588–598.
- [10] J.R. Szczech, S. Jin, Energy Environ. Sci. 4 (2011) 56–72.
- [11] H. Zhao, Z. Zheng, K.W. Wong, S. Wang, B. Huang, D. Li, Electrochem. Commun. 9 (2007) 2606–2610.
- [12] N. Sharma, K.M. Shaju, G.V. Subba Rao, B.V.R. Chowdari, J. Power Sources 124 (2003) 204–212.
- [13] Y.N. NuLi, Q.Z. Qin, J. Power Sources 142 (2005) 292–297.
- [14] Z.H. Li, T.P. Zhao, X.Y. Zhan, D.S. Gao, Q.Z. Xiao, G.T. Lei, Electrochim. Acta 55 (2010) 4594–4598.
- [15] S.L. Kuo, N.L. Wu, Electrochem. Solid State Lett. 10 (2007) A171–A175.
- [16] R. Kalai Selvan, N. Kalaiselvi, C.O. Augustin, C.H. Doh, C. Sanjeeviraja, J. Power Sources 157 (2006) 522–527.
- [17] Y. Ding, Y.F. Yang, H.X. Shao, Electrochim. Acta 56 (2011) 9433–9438.
- [18] C. Vidal-Abarca, P. Lavela, J.L. Tirado, J. Phys. Chem. C 114 (2010) 12828–12832.
- [19] X.D. Li, W.S. Yang, F. Li, D.G. Evans, X. Duan, J. Phys. Chem. Solids 67 (2006) 1286–1290.
- [20] P. Lavela, J.L. Tirado, J. Power Sources 172 (2007) 379–387.
- [21] A. Manthiram, A. Vadivel Murugan, A. Sarkar, T. Muraliganth, Energy Environ. Sci. 1 (2008) 621–638.
- [22] N. Jayaprakash, W.D. Jones, S.S. Moganty, L.A. Archer, J. Power Sources 200 (2012) 53–58.
- [23] J. Xie, X. Yang, S. Zhou, D. Wang, ACS Nano 5 (2011) 9225–9231.
- [24] W.M. Zhang, X.L. Wu, J.S. Hu, Y.G. Guo, L.J. Wan, Adv. Funct. Mater. 18 (2008) 3941–3946.
- [25] J.H. Lin, T.H. Ko, W.S. Kuo, C.H. Wei, Energy Fuels 24 (2010) 4090–4094.
- [26] J. Wang, X. Sun, Energy Environ. Sci. 5 (2012) 5163–5185.
- [27] Y. Liu, X. Zhao, F. Li, D. Xia, Electrochim. Acta 56 (2011) 6448–6452.
- [28] Y. Ding, Y.F. Yang, H.X. Shao, Solid State Ionics 217 (2012) 27–33.
- [29] Z.L. Wang, X.J. Liu, M.F. Lv, P. Chai, Y. Liu, J. Meng, J. Phys. Chem. B 112 (2008) 11292–11297.
- [30] Y.F. Deng, Q.M. Zhang, S.D. Tang, L.T. Zhang, S.N. Deng, Z.C. Shi, G.H. Chen, Chem. Commun. 47 (2011) 6828–6830.
- [31] R. Alcántara, M. Jaraba, P. Lavela, J.L. Tirado, J.C. Jumas, J. Olivier-Fourcade, Electrochem. Commun. 5 (2003) 16–21.